Journal of Visualized Experiments

Induction of Microstreaming by Nonspherical Bubble Oscillations in an Acoustic Levitation System

--Manuscript Draft--

Article Type:	Invited Methods Article - JoVE Produced Video
Manuscript Number:	JoVE62044R1
Full Title:	Induction of Microstreaming by Nonspherical Bubble Oscillations in an Acoustic Levitation System
Corresponding Author:	Claude Inserra, Ph.D. Universite de Lyon Lyon, France FRANCE
Corresponding Author's Institution:	Universite de Lyon
Corresponding Author E-Mail:	claude.inserra@inserm.fr
Order of Authors:	Claude Inserra, Ph.D.
	Gabriel Regnault
	Sarah Cleve
	Cyril Mauger
	Philippe Blanc-Benon
Additional Information:	
Question	**Response**
Please specify the section of the submitted manuscript.	Engineering
Please indicate whether this article will be Standard Access or Open Access.	Standard Access (US$2,400)
Please indicate the **city, state/province, and country** where this article will be **filmed**. Please do not use abbreviations.	Lyon, France
Please confirm that you have read and agree to the terms and conditions of the author license agreement that applies below:	I agree to the Author License Agreement
Please provide any comments to the journal here.	

TITLE:

Induction of Microstreaming by Nonspherical Bubble Oscillations in an Acoustic Levitation System

AUTHORS AND AFFILIATIONS:

Claude Inserra[1], Gabriel Regnault[2], Sarah Cleve[2], Cyril Mauger[2], Philippe Blanc-Benon[2]

[1] Univ Lyon, Université Claude Bernard Lyon 1, Centre Léon Bérard, INSERM, UMR 1032, LabTAU, Lyon, France

[2] Univ Lyon, Ecole Centrale de Lyon, INSA de Lyon, CNRS, LMFA UMR 5509, Ecully, France

Corresponding Author:

Claude Inserra (claude.inserra@inserm.fr)

E-mail Addresses of Co-authors:

Gabriel Regnault (gabriel.regnault@insa-lyon.fr)

Sarah Cleve (s.cleve@utwente.nl)

Cyril Mauger (cyril.mauger@insa-lyon.fr)

Philippe Blanc-Benon (philippe.blanc-benon@ec-lyon.fr)

KEYWORDS:

Cavitation, microbubble, shape oscillations, microstreaming, high-speed imaging, bubble coalescence

SUMMARY:

A fast and reliable technique is proposed to control the shape oscillations of a single, trapped acoustic bubble that is based on coalescence technique between two bubbles. The steady-state, symmetry-controlled bubble shape oscillations allow analysis of the fluid flow generated in the vicinity of the bubble interface.

ABSTRACT:

When located near biological barriers, oscillating microbubbles may increase cell membrane permeability, allowing for drug and gene internalization. Experimental observations suggest that the temporary permeabilization of these barriers may be due to shear stress that is exerted on cell tissues by cavitation microstreaming. Cavitation microstreaming is the generation of vortex flows which arise around oscillating ultrasound microbubbles. To produce such liquid flows, bubble oscillations must deviate from purely spherical oscillations and include either a translational instability or shape modes. Experimental studies of bubble-induced flows and shear stress on nearby surfaces are often restricted in their scope due to the difficulty of capturing shape deformations of microbubbles in a stable and controllable manner. We describe the design of an acoustic levitation chamber for the study of symmetry-controlled nonspherical oscillations. Such control is performed by using a coalescence technique between two approaching bubbles in a sufficiently intense ultrasound field. The control of nonspherical oscillations opens the way to a controlled cavitation microstreaming of a free surface-oscillating microbubble. High-frame

rate cameras allow investigating quasi-simultaneously the nonspherical bubble dynamics at the acoustic timescale and the liquid flow at a lower timescale. It is shown that a large variety of fluid patterns may be obtained and that they are correlated to the modal content of the bubble interface. We demonstrate that even the high-order shape modes can create large-distance fluid patterns if the interface dynamics contain several modes, highlighting the potential of nonspherical oscillations for targeted and localized drug delivery.

INTRODUCTION:

In medicine, an administered drug must penetrate many obstacles in the living system before reaching the desired targets. However, most drugs are rapidly cleaned away from the blood stream. The targeting efficiency is low and they cannot easily cross cell membranes, leading to ineffective drug delivery. Currently, the use of microbubbles in combination with ultrasound has been proposed as an innovative method for noninvasive, precise and targeted delivery of drugs and genes to pathological tissues and cells[1]. In this approach, microbubbles can play a role as carriers where free drugs are either co-injected with a gas bubble suspension or loaded on its surface. Microbubbles can also act as a local vector for refocusing the ultrasound energy in order to interact with the cells. Basically, under ultrasound exposure, bubbles stably compress and expand, a regime called stable cavitation that generates liquid flows and hence shear stress on nearby objects. Microbubbles may also oscillate non-linearly and expand until collapse, in the regime of inertial cavitation, producing shock waves that propagate radially from the collapse site[2]. It has been shown that cavitation, either stable or inertial, enhances the permeabilization of cell membranes, and thus enhances the internalization of drugs into the cell[3].

In therapeutic applications, understanding the mechanism of the bubble-cell interaction is very important, but there are several barriers, both from scientific and technical sides, that prevent our knowledge from advancing. First, capturing the dynamics of cells in response to bubble-induced mechanical stimuli is very difficult[4]. At the acoustic timescale, the first-order microbubble oscillations can lead to activation of membrane channels, facilitating molecular passage across biological interfaces. This occurs through the direct oscillation of the cell membrane, also called “cellular massage”[5]. Channel activation following direct mechanical stress was evidenced using patch-clamp techniques that measured electrophysiological properties of cell membranes during and after ultrasound exposure[6]. Measuring bubble-induced cell dynamics (meaning the complete field of deformation of the cell membrane) at the acoustic timescale, would also provide insights in the threshold of membrane area expansion $\Delta A/A$ required to induce pores into the cell membrane[7]. The second barrier is controlling the collapsing bubble regime to avoid microbubble-induced cell lysis. Bubble collapses and induced microjets have been identified as a mechanism through which membrane perforation occurs[8,9]. Once permeabilized, the cell membrane repairs through calcium self-sealing of the lipid bilayers and fusion of intracellular vesicles[9]. The occurrence of bubble collapses may also cause lethal damages to the cell and induce unnecessary side effects in the surrounding ones. In sensitive applications such as ultrasound-mediated blood-brain barrier opening, it is generally accepted that inertial bubble collapses should be avoided[10].

Therefore, huge efforts are currently devoted to the design of ultrasound emission sequences,

coupled with passive cavitation monitoring and control, in order to ensure stable oscillations of microbubbles[11]. In this stable regime, it has been hypothesized that stably oscillating bubbles play a strong role in the triggering of membrane permeabilization by promoting spatially-targeted shear stress on the cell membrane[7]. The shear stress results from the liquid flows created in the vicinity of the oscillating bubbles. These liquid flows are called cavitation microstreaming, and, as mentioned above, they are one of the several possible mechanisms which are responsible for enhanced uptake of extracellular molecules. When dealing with suspension of bubbles or cells such as in-vitro biological transfections assays[12], permeabilization by microstreaming might be much more efficient than permeabilization by bubble collapse. This can be shown by a simple geometrical consideration. In cell suspensions, sonoporation will be efficient if the majority of the suspended cells is submitted to sufficiently large mechanical effects (leading to membrane permeabilization). It is known that bubble collapses are directed along the direction of isotropic symmetry breaking, such as the bubble-wall axis[13] or the bubble-bubble and bubble-cell line joining their center of mass[14]. The produced microjet is therefore a spatially-localized phenomenon along a finite number of lines joining the cell and bubble centers. Depending on the cell and bubble concentration, as well as the bubble-cell distance, this effect may not be the most efficient to permeabilize the whole number of suspended cells. In contrast, cavitation microstreaming is a phenomenon occurring at a slow timescale, with a large spatial expansion in comparison to the bubble radius. Also, the liquid flow is distributed all around the bubble, and may therefore impacts a larger number of cells, at a very long range. Therefore, understanding the generated cavitation microstreaming around an oscillating bubble is a prerequisite for controlling and quantifying the bubble-induced shear stress that is applied to cells.

To do so, a preliminary step consists in controlling the spherical and nonspherical oscillations of an ultrasound-driven bubble, as the generated liquid flows are induced by the motion of the bubble interface[15,16]. In particular, shape oscillations of microbubbles have to be triggered and kept stable. Furthermore, the orientation of the bubble shape oscillations has to be controlled to properly analyze the correlation between the bubble interface dynamics and the induced microstreaming pattern. When summarizing the existing literature, it is obvious that detailed experimental results of cavitation-induced microstreaming are only available for bubbles attached to a surface. Wall-attached microbubbles are commonly-used for assessing accurate interface dynamics and cell interactions at the micrometer scale under an ultrafast microscopy system. This configuration is therapeutically relevant when considering vibrating microbubbles located on the cell membrane[17,18,19]. The study of substrate-attached bubble may however make the analysis of bubble dynamics more complicated, partly due to the complex nature of contact line dynamics[20], and the triggering of asymmetric shape modes[21]. In medical and biological applications, bubbles that are not attached to a wall are commonly found in confined geometries such as small vessels. This impacts significantly bubble dynamics and shape instabilities. Particularly, the presence of a nearby wall shifts the pressure threshold for shape mode triggering to lower pressure values depending on the shape mode number and bubble size[22]. The wall also affects the bubble-induced microstreaming with possibly higher intensity for the produced flow[23].

Amongst all the possible scenario that microbubbles may experience (free or attached, close to a wall, collapsing or stably-oscillating), we propose to investigate the nonspherical dynamics of a single bubble far from any boundary. The experimental setup is based on an acoustic levitation system[24] in which a standing ultrasound wave is used to trap the bubble. This scenario is consistent with medical applications in which a collection of suspended bubbles and cells coexist in a sonotransfection chamber, for instance. As far as bubbles and cells are not too close, it is assumed that the presence of a cell does not impact the bubble interface dynamics. When cells follow the loop-like trajectories of the cavitation-induced microstreaming, they are cyclically approaching and repelling from the bubble location and we can assume that the cell presence impacts neither the streaming pattern nor its mean velocity. In addition, nonspherical dynamics and induced microstreaming from single bubbles far from boundary are well known from a theoretical point of view. In order to link the bubble-induced liquid flow to the bubble contour dynamics, it is required to accurately characterize the bubble interface dynamics. To do so, it is preferable to adapt the spatiotemporal scale in experimental studies with respect to those used in therapeutics so that acquisition with common high-speed cameras (below 1 million frame/second) is possible by using large bubbles excited at lower frequencies. When considering uncoated bubbles, the eigenfrequency ω_n of a given mode n is related to the bubble size as $\omega_n^2 R_0^2 \sim Constant$[25]. This radius-eigenfrequency relationship is slightly modified when considering shelled bubbles[26], but the order of magnitude of the eigenfrequency ω_n remains the same. Thus, investigating bubbles with equilibrium radii $\sim 50\mu m$ in a 30 kHz ultrasound field is similar to studying coated bubbles of radii $\sim 3\mu m$ in a 1.7 MHz field, as proposed by Dollet et al.[27]. Similar shape mode numbers and hence microstreaming patterns are therefore expected.

In order to trigger nonspherical oscillations of the bubble interface, it is necessary to exceed a certain pressure threshold that is radius-dependent, as shown in **Figure 1**. Existing experimental techniques rely on the increase of the acoustic pressure to trigger surface modes (illustrated by path (1) in **Figure 1**), either by step-by-step pressure increase[28] or by modulated-amplitude excitation responsible of periodic onset and extinction of surface modes[29]. The main drawbacks of these techniques are (i) a random orientation of the symmetry axis of the surface oscillations that cannot be controlled to be in the imaging plane, (ii) a short lifetime of the bubble shape oscillations that makes the analysis of the induced liquid flows difficult at larger timescales, and (iii) the frequent triggering of unstable shape modes. We propose an alternative technique to cross the pressure threshold at a constant acoustic pressure in the radius/pressure map, as illustrated by the path (2) in **Figure 1**. To do so, it is required to increase the bubble size such that it will be in the instability zone. Such an increase is performed by a bubble coalescence technique. The coalescence of two, initially spherically-oscillating, microbubbles is exploited to create one single deformed bubble. If the acoustic pressure and bubble size of the coalesced bubble are in the instability zone, surface modes are triggered. We also evidenced that the coalescence technique induces stable shape oscillations in a steady-state regime, as well as a controlled symmetry axis defined by the rectilinear motion of the two approaching bubbles. Because a stable shape oscillation is ensured over minutes, the analysis of bubble-induced fluid flow is possible by seeding the liquid medium with fluorescent microparticles, lighted by a thin laser sheet. Recording the motion of the solid microparticles in the vicinity of the bubble interface allows identifying the pattern of the induced fluid flow[30]. The overall principle of the triggering

of bubble shape oscillations, leading to a time-stable fluid flow, is illustrated in **Figure 2**.

In the following protocol, we outline the steps required to create stable bubble shape oscillations via the coalescence technique and describe the measurements of fluid flow. This includes the design of the acoustic levitation system, the acoustic calibration, bubble nucleation and the coalescence technique, the measurement of bubble interface dynamics and surrounding fluid flow, and the image processing.

PROTOCOL:

1. Design of the acoustic levitation chamber

1.1. Design an optically transparent (PMMA-like) cubic tank (8 cm edge and 2.8 mm thickness per face) with the geometry module of a multiphysics simulation software (**Table of Materials**).

1.2. Insert a cylindrical surface (Ø = 35 mm) centered at the bottom of the tank, to model the ultrasonic transducer.

1.3. Set the boundary conditions to zero pressure on each wall with a normal displacement of amplitude 1 µm at the transducer surface.

1.4. Using a Frequency domain module, simulate the Frequency Response Function (FRF) of the tank in the frequency range [10 - 40] kHz, at the three arbitrary locations loc1 = (0.01375, 0.01375, 0.04125), loc2 = (0, 0, 0.0088), and loc3 = (0.021725, 0.023375, 0.00935).

1.5. Adapt the tank size such that one of the acoustic modes of the cavity corresponds to the nominal frequency of the transducer (here 31.2 kHz). The FRF therefore contains one resonance peak close to this frequency, as illustrated in **Figure 3**.

1.6. Plot the pressure field inside the tank, as shown in **Figure 4**. The chosen resonance mode must contain at least one pressure antinode in the inner of the container, on which the acoustic bubble will be trapped.

1.7. When designing the tank, design a movable top face with a guiding groove on each edge to tightly close the tank faces. Drill a tiny hole at the top face in order to fill the tank with the liquid medium.

1.8. Place the water tank atop a homemade frame that contains the ultrasound transducer (Langevin-type, 31.2 kHz nominal frequency). Use echographic gel to couple the transducer to the tank bottom wall.

1.9. Place the tank and frame system atop a three-directions displacement table with micrometric screws.

1.10. Fill the tank with microfiltered, demineralized and water (not degassed, volume ~500mL, oxygen saturation of approximatively 8 $mg \cdot L^{-1}$).

NOTE: Using not degassed water instead of degassed makes it possible to maintaining stable bubbles for the duration of experiments. Using degassed water will accelerate bubble shrinking due to gas diffusion, even if slightly counterbalanced by rectified (ultrasound-mediated) diffusion.

2. Bubble generation and acoustic calibration

2.1. Prepare the experimental setup used for laser-induced bubble nucleation, acoustic excitation and high-speed recording (**Figure 5a,b,c**). The experimental setup consists of (A) the acoustic levitation system, (B) the laser power supply and (C) the laser head, (D) one spherical concave lens, (E) one plano-concave lens and one aspherical lens, (F) the high-speed camera, (G) the continuous light-emitting diode. Later, for measurements of liquid flows (**Figure 5d**) (H) one continuous wave laser source, (I) a cylindrical plano-concave lens followed by a cylindrical plano-concave lens inserted behind the first lens and oriented on the orthogonal axis will be added.

2.2. Plug the ultrasound transducer to a function generator. Set the excitation signal as: sinusoidal waveform, continuous wave, frequency 31.2 kHz. The amplitude is the only variable parameter.

2.3. Place the lens (D) at a distance of approximatively 6 cm in front of the laser head (C).

2.4. Place the lens (E) at a distance of approximatively 12 cm in front of the lens (D).

2.5. Place the water tank (A) such that a focusing point of the laser is located inside the water tank, leading to spark generation for every laser pulse (5 -10 mJ). The laser spark should be located approximately 3 cm below the targeted pressure antinode.

NOTE: Without ultrasound (US), laser-nucleated bubble will rise to the top face due to buoyancy.

2.6. Switch on the ultrasound transducer. Increase the applied voltage until the bubble no longer rises vertically but is deviated towards the pressure antinode and, for a sufficient high pressure, trapped.

2.7. Set the backlit illumination (continuous light-emitting diode) and the high-speed camera in order to observe the trapped bubble.

NOTE: When nucleating a new bubble with a laser spark, it is easy to capture the trajectory of the bubble approaching its trapping location.

2.8. Move the location of the laser spark within the water tank such that the bubble trajectory remains inside the focal plane of the camera.

2.9. Trap one bubble and capture its radial oscillations with the following parameters: frame size 128 x 128 pixels, acquisition rate 180 kHz. An example of large-amplitude radial oscillations over two acoustic periods is provided in **Figure 6**. Typical gas bubbles size ranges from 30 to 80 µm.

2.10. Record the bubble radial oscillations during 3 to 30 milliseconds in order to capture hundreds to thousands of bubble oscillations. Repeat this recording for increasing applied voltages of the transducer. Typical applied voltages are in the range of 0 – 8 V.

NOTE: When modifying the applied voltage, the equilibrium location of the trapped bubble slightly moves vertically. To follow the oscillations without moving the backlit illumination and camera, place the system (transducer and water tank) onto a three-directions movable table with micrometric accuracy.

2.11. Switch on the ultrasound transducer and capture one image of the background for post-analysis.

2.12. Post-process the video series following this procedure:

2.12.1. Run the executable file VoltagePressure.exe. The interface shown in **Figure 7** should open.

NOTE: The script is available as a supplementary document.

2.12.2. Specify the physical and experimental parameters in the left column (**Figure 7A**).

2.12.3. Specify the values of applied voltage for the series of recordings in the bottom-right table (**Figure 7B**).

2.12.4. In the **Bubble radius analysis** panel, click on **Load parameters** (**Figure 7C**) and select the folder containing all the files of your video series, and then the background image (mandatory).

2.12.5. The choice is allowed between analyzing all the videos at once, by clicking on **Auto**, or one-by-one by clicking on **Step by step**.

2.12.6. For each video file, the evolution of the bubble radius is plotted over one acoustic period, and a numerical fit is superimposed. The red curve corresponds to a linearized Rayleigh-Plesset modeling. The equilibrium bubble radius is displayed (**Figure 7D**).

2.12.7. According to the numerical fitting, the applied pressure for this voltage is displayed in the **Pressure (Voltage) graph** panel (**Figure 7E**). The value of the applied pressure is also displayed in the bottom-right table (**Figure 7B**). Typical applied pressures corresponding to the 0 – 8 V voltage dynamics are 0 – 25 kPa.

2.12.8. Once all videos are processed, click on the **Linear regression** button to perform a linear fit of the pressure/voltage curve. The data (voltage and pressure values) are saved into a .txt file located in the current directory. The slope of the fit is provided.

3. Coalescence technique

3.1. Switch on the ultrasound transducer. Set the applied voltage high enough such that the corresponding acoustic pressure may lead to the triggering of surface instability, according to the numerical pressure/radius diagram of instability zones, as shown in **Figure 8**.

3.2. Nucleate a bubble, which will then migrate to its trapping location. If the trapped bubble only exhibits spherical oscillations, move on to the next step. If nonspherical oscillations appear:

3.2.1. Switch off the ultrasound power to let the bubble rise to the top surface.

3.2.2. Modify the laser energy (by finely tuning over a few mJ) or reduce the transducer voltage.

3.2.3. Switch on the ultrasound power.

3.2.4. Nucleate a new bubble.

3.2.5. Repeat this procedure until the bubble size leads to purely spherical oscillations.

3.3. When a trapped bubble exhibits only spherical oscillations, generate a new laser spark. When the new bubble reaches the trapping location, coalescence occurs.

3.4. If the coalesced bubble exhibits only spherical oscillations, generate a new bubble. Multiple coalescences may be necessary to reach the bubble radius at which nonspherical deformations occur. An example of bubble coalescence leading to nonspherical oscillations is shown in **Figure 9**.

3.5. Once the coalesced bubble exhibits nonspherical oscillations, record the bubble oscillations for a duration of approximatively 3 to 30 milliseconds.

3.6. Identify the mode number of shape oscillations by referring to **Figure 10**.

4. Fluid flow measurements

4.1. In the case of cavitation microstreaming measurements, fluorescent tracer particles must be added to the water prior to bubble nucleation. In this study, 0.71 µm particles are used (**Table of Materials**). They are sufficiently small to be acoustically transparent (not influenced by the acoustic radiation force) and to accurately follow the flow as well as sufficiently large to scatter laser light. Use three drops for the volume of the water tank, corresponding to approximatively 2.10^4 particles/mm^3.

4.2. Prior to taking measurements, set the following parameters for capturing both the (fast timescale) bubble dynamics and (low timescale) fluid flow:

4.2.1. Create a partitioning of the camera recording disk.

4.2.2. Alternatively define the recording parameters as:

4.2.2.1. Frame rate 180 kHz, frame size 128 x 128 pixels, and exposure time 1 µs for one recording of the dynamics of the bubble interface

4.2.2.2. Frame rate 600 Hz, frame size 1024 x 768 pixels, and exposure time 1 ms for one recording of the motion of dye tracers.

4.3. Use a continuous laser.

4.4. Create a thin laser sheet by successively letting the laser beam pass through cylindrical plano-concave lens and cylindrical plano-convex lens oriented on an orthogonal axis. A beam width of about 160 µm can be obtained.

4.5. Set up the laser sheet to correspond to the imaging plane:

4.5.1. Set the laser on a movable device so that the laser sheet can be moved parallel to the imaging plane.

4.5.2. Adjust the position so that the illuminated particles are visible by the camera.

4.5.3. Nucleate and trap a bubble.

4.5.4. Adjust the position of the laser sheet further, so that a shadow becomes visible behind the bubble. The bubble is now inside the laser sheet, as shown in **Figure 11**.

4.6. Induce bubble coalescence until a stably oscillating shape mode is apparent.

4.7. Do several recordings switching back and forth between bubble dynamics and microstreaming.

NOTE: Switch off the continuous laser when not needed. Heating can create unwanted convective flows. Also, turn off the light-emitting diode when performing the measurements of streaming flow.

5. Image processing to visualize the cavitation microstreaming patterns

5.1. Install the visualization software ImageJ for image processing and analysis in Java. Also

install the plugin CINE File Reader in order to open the high-speed camera files.

5.2. Click on **File | Import | CineFile** and select the video *.cine containing the capture of the particle motion.

5.3. Select **Use virtual stack** in the new window, the video is now loaded.

5.4. In order to observe the particle motion without displaying the streaming pattern, click on **Image | Adjust | Brightness/Contrast | Auto**. The dark background is now replaced by an automatically optimized image.

5.5. In order to display the resulting pattern, click on **Image | Stacks | Z Project** and choose the **Max Intensity** option for the image projection. An output image with pixels containing the maximum value over all images in the stack is displayed. Adjust the image contrast as described in step 5.4, if necessary.

NOTE: A streaming pattern such as the ones shown in **Figure 12b** and **Figure 12d** is obtained.

REPRESENTATIVE RESULTS:

A complete sequence of bubble coalescence leading to time-stable, symmetry-controlled nonspherical oscillations is presented in **Figure 9**. The approaching phase of two spherically-oscillating bubbles ends when the thin liquid film between the two bubbles is ruptured. It is worth noting that, at the last stage prior to the coalescence, the bubble interfaces deviate from sphericity. Both bubbles elongate on an ellipsoidal shape along the path of the rectilinear motion of approach. After the moment of coalescence, a single bubble remains and exhibits nonspherical oscillations with a complex shape during a few acoustic periods. This corresponds to the transient regime of oscillations, following the excitation of any dynamical system. After a dozen to a hundred acoustic periods the shape oscillations stabilize on a steady-state oscillation, here shown for a mode 4, as can be deduced from the interpretation of **Figure 10**. This mode may persist for thousands of acoustic periods, for several milliseconds to a few minutes. This allows the quasi-simultaneous measurements of bubble-induced liquid flows.

Once a bubble is trapped and exhibits steady shape oscillations, the motion of fluorescent tracers in the bubble vicinity is captured, as shown in **Figure 11**. First of all, the absence of particle motion for a bubble exhibiting purely spherical oscillations is consistent with several cavitation microstreaming models[31] which evidence that no vorticity is induced by pure radial oscillations. When shape oscillations occur, liquid motion is produced in the vicinity of the bubble interface, as shown in **Figure 12**. The alternative recording of the dynamics of the bubble interface at the acoustic timescale (**Figure 12a,c**) and of the motion of particles at a lower timescale (**Figure 12b,d**) allows correlating the microstreaming pattern to a given shape mode number. **Figure 12a** presents a snapshot series of the bubble dynamics for a bubble of mean radius R_0=70.5 µm, driven at the acoustic pressure P_a=12.8 kPa, which is oscillating predominantly on a mode 3. The associated microstreaming pattern, in **Figure 12b**, consists of six lobes. The conservation of the axis of symmetry between shape mode oscillations and the microstreaming pattern is clearly

visible. **Figure 12c** presents a snapshot series of the bubble dynamics for a bubble of mean radius R_0=55.7 µm, driven at the acoustic pressure P_a=23.6 kPa, which is oscillating predominantly on a mode 4. The associated microstreaming pattern in **Figure 12d** consists of eight small lobes of the size of the bubble diameter. Once more, the conservation of the axis of symmetry between shape mode oscillations and the microstreaming pattern is clearly visible. These results seem to confirm that the higher-order the shape modes the smaller the microstreaming pattern and the more confined they are in the bubble vicinity.

This assumption of a narrower streaming pattern for higher-order modes is not as obvious and depends on the modal content of the bubble interface dynamics. Indeed, we must recall that bubble-induced liquid flow results from the interactions between two shape modes oscillating at the same frequency, or the self-interaction of a mode with itself[31]. A bubble oscillating predominantly on a given shape mode, for instance let us consider a mode 3, may also excite other nonspherical oscillations through nonlinear coupling between modes[29]. If the dynamics of the bubble interface contain supplementary modes, such as the second and fourth one (for instance), then the microstreaming flow can be significantly modified due to the multiple interactions between modes that would generate specific patterns. This is illustrated in **Figure 13** for two bubbles oscillating predominantly on a mode 3, that induce two different microstreaming patterns. In **Figure 13a**,**b**,**c**, a bubble of equilibrium radius R_0 = 70.1 µm, driven at the acoustic pressure P_a=12.4 kPa, oscillating on a mode 3, presents a lobe-type pattern. Analysis of the interface dynamics (**Figure 13b**) reveals that the predominant modes are the radial one (oscillating at the driving frequency f_0), the translational one (mode with number 1, oscillating at half the driving frequency f_0), the third one (oscillating at $f_0/2$) and a relatively small fourth and sixth modes (both oscillating at f_0). It can be hypothesized that the main contribution to the microstreaming flow is the interaction between the radial mode and mode 4 and 6, leading to a lobe-type pattern[31]. In **Figure 13d**,**e**,**f**, a bubble of equilibrium radius R_0 = 68.6 µm, driven at the acoustic pressure P_a = 13.3 kPa, oscillating on mode 3, presents a cross-type pattern, with large-distance flow extension. The analysis of the interface dynamics (**Figure 13d**) reveals that the predominant modes are the radial one, the translational one (mode with number 1), the third and the sixth one. According to the high amplitude of mode 3, it can be hypothesized that the main contribution to the microstreaming flow is the self-interaction of mode 3, leading to a cross-type pattern[32].

FIGURE AND TABLE LEGENDS:

Figure 1. Illustration of the method for triggering shape oscillations. The pressure/radius map contains one instability zone per mode of a given degree. The pressure threshold to reach this zone can be crossed by (1) increasing the applied acoustic pressure that drives a gas bubble of fixed radius, until shape modes appear, or (2) increasing the bubble size at a constant applied acoustic pressure. Such increase in the bubble volume happens slowly when rectified diffusion occurs, while bubble coalescence significantly fastens the process.

Figure 2. Illustration of the bubble coalescence technique. The approaching phase (A) consists of laser-nucleating two bubbles that encounter each other at the same trapping location within the container. When they meet, coalescence occurs: rupture of the thin liquid film between

bubbles (B) leads to the generation of a single, initially-deformed, bubble. This deformed bubble is driven by the monochromatic ultrasound field and exhibits at first transient oscillations (C), before entering the steady-state regime. In the steady-state regime (D), the coalesced bubble exhibits time-stable, symmetry-controlled shape oscillations. By seeding the medium with fluorescent nanoparticles, the bubble-induced fluid flow is captured (E).

Figure 3. Frequency Response Function of the pressure field within the levitation system. The amplitude of the acoustic pressure is displayed as a function of the frequency, for three locations inside the tank corresponding to the following (x,y,z) coordinates: (1) blue, (2.05,2.05,6)cm, (2) red, (0,0,1.28)cm and (3) black, (3.23,3.48,1.36)cm, where the origin of the coordinate system is taken at the center of the bottom face of the cubic tank. Near 31.5kHz a resonance mode is clearly visible.

Figure 4. Distribution of the acoustic pressure within the levitation chamber. (A) Three-dimensional representation of the pressure field within the cubic water tank for the selected resonance mode. This mode occurs at the frequency 31.2 kHz corresponding to the frequency of the ultrasound source. (B) Distribution of the acoustic pressure in the diagonal plane of the tank. (C) Distribution of the acoustic pressure in a horizontal (height z=constant) plane. The altitude has been chosen such that it corresponds to the location of the pressure antinode in the upper part of the tank. The amplitudes of the color bar are obtained by imposing a normal displacement of 1 μm at the transducer surface.

Figure 5. Photographs and schematics of the experimental setup. It is constituted of (A) the acoustic levitation system, (B-C) the pulsed laser amplifier and laser head, (D-E) the focusing lens set, (F) the high-speed camera, (G) the light-emitting diode, (H) the continuous wave laser and (I) the shaping lens set. (a) A side and (b) a top view of the experimental setup. (c) Illustration of the materials required for capturing the bubble oscillations. Note that the continuous laser (H) is switched off during this process. (d) Illustration of the materials required for capturing the liquid flows. Note that the pulsed laser (C) for bubble nucleation is switched off, while the continuous laser (H) for generating a laser sheet illuminating the microparticle tracers is on.

Figure 6. Snapshot series of an ultrasound-driven bubble exhibiting large amplitude spherical oscillations. The bubble equilibrium radius is ~60 μm, and the driving acoustic pressure is ~15 kPa. The time interval between two successive images is 5.6 μs. The entire series corresponds to two acoustic periods.

Figure 7. Interface panel of the executable script PVR_Interface.exe. The script launches a Graphical User Interface that contains (A) a panel for setting the physical parameters, (B) a table for setting the applied electrical voltage applied to the transducers, (C) the possibility of loading the whole set of recorded videos that are post-processed and provide the equilibrium bubble radius (D) and the applied acoustic pressure (B), the plot of the pressure/voltage relationship (E).

Figure 8. Pressure/radius diagram of instability zones. Each colored area corresponds to an instability zone for a given shape mode: (blue area) Mode 2, (green area) Mode 3 and (red area)

Mode 4. The white area corresponds to the case where microbubbles exhibit only spherical oscillations.

Figure 9. Snapshot series of a bubble coalescence leading to shape oscillations. After the approaching phase of two bubbles, the thin film between them is ruptured and coalescence occurs. A single bubble is now driven by the ultrasound field, first in a transient oscillation regime. After some acoustic periods the steady-state regime is established on an axisymmetric shape mode, here the mode 4. The time interval between two successive photographs is 30 µs.

Figure 10. The first five axisymmetric shape modes, including the radial mode. Side-view of the contour of the bubble interface shown at two extrema of the oscillation amplitude.

Figure 11. Fluorescent tracer particles around spherically-oscillating microbubbles. Both images correspond to a superposition of 100 snapshots covering 0.25s. (a) No motion of the tracer particles can be observed if shape oscillations are not present. (b) A parasite mean flow visible in the whole field of view can appear for instance due to heating of the lase sheet. This flow is however not linked to the bubble motion. On both images the shadow induced by the laser sheet behind the bubble is clearly visible.

Figure 12. Quasi-simultaneous recording of the bubble dynamics and the induced microstreaming. Left column: Snapshot series of one bubble exhibiting shape mode oscillations of order 3 (a) and the induced microstreaming (b). Right column: Snapshot series of one bubble exhibiting shape mode oscillations of order 4 (c) and the induced microstreaming (d). For all figures the red dashed line corresponds to the symmetry axis of both the bubble shape oscillations and liquid flows, determined by the rectilinear motion of the two approaching bubbles prior to coalescence.

Figure 13. Example of two streaming patterns induced by a bubble oscillating predominantly on a mode 3. (a,d) Illustration and snaphot of the bubble interface, (b,e) the mode decomposition of the bubble interface and (c,f) the associated streaming pattern.

DISCUSSION:

The presented procedure consists of using bubble coalescence in order to trigger steady-state, symmetry-controlled bubble shape oscillations, allowing the study of the long-term fluid flow induced by these oscillations. The main challenge in the technique is the control of nonspherical oscillations for a bubble being trapped, far from any boundaries.

Most of the existing techniques proposed in the literature focused on substrate-attached bubbles[7,16], as the absence of motion of the bubble center makes the capture of its interface at the acoustic timescale (up to hundreds of kHz) easier. While exceeding the pressure threshold necessary to trigger shape modes is an easy task in this case, the control of shape oscillations is complicated due to the break of symmetry induced by the substrate. A wall-attached bubble is contacting the substrate with a particular contact angle, leading to the triggering of asymmetric surface modes[21]. In addition to the complexity of interpreting the three-dimensional, asymmetric

modes with only a single camera view, abrupt transition to a chaotic surface oscillation regime arises[33]. Therefore, the main challenge consists in capturing shape oscillations of a single, trapped bubble far from any boundaries in order to obtain axisymmetric nonspherical oscillations. Such conditions enable comparison between experiments and the large variety of analytical studies available in literature. The main experimental difficulty lies in the positional stability of the microbubble. To overcome this problem, optical tweezers have been used to control bubble trapping[34], and amplitude-modulated ultrasound fields are used to trap and drive bubble oscillations[29]. In both cases, a single bubble is trapped and nonspherical modes are triggered. Also, in the case of the amplitude-modulated driving field, the shape modes only exist for a small period of time as they periodically onset and disappear. In addition, the orientation of bubble shape oscillations is not controlled and leads to a bias in the analysis of the interface motion.

The alternative we propose is the use of a pulsed laser to nucleate a single bubble, later trapped at a pressure antinode of a resonance levitation chamber. By nucleating successive bubbles over time, each nucleated bubble moves towards its trapping location which is already occupied by another bubble. Coalescence occurs and induces an initially-deformed bubble interface. If the driving pressure is sufficiently strong, the shape oscillations are sustained. Laser-nucleation has been preferred to other nucleation techniques, such as electrolysis for instance, as it allows fast and reliable bubble generation. As illustrated in **Figure 9**, the axis of symmetry of shape oscillations is given by the axis of bubble approach prior to coalescence. However, this major result requires a relatively long time for setting the experimental setup as it is required that the bubbles stay inside the focal plane of the camera during the approach phase of coalescence (in order to orient the axis of symmetry in this plane). To do so, slight changes of the bubble nucleation site are made in order to optimize the path along which the bubbles move and encounter each other. The change into bubble-nucleation site requires fine modification of the tank location relatively to the laser path, and is performed with a three-directions stage with micrometric accuracy. In addition, fine tuning of the laser energy is performed in order to optimize the nucleated bubble size. Bubbles that are too large will immediately generate shape modes with high mode number and approach the volumetric bubble resonance. This leads to high positional instability of the bubble center. Bubbles that are too small will require a large number of coalescence processes before reaching the appropriate size for triggering shape modes.

The main advantage of the proposed technique is the establishment of a steady-state regime for symmetry-controlled shape oscillations. As the interface motion is sustained for a relatively long time (from seconds to minutes), capturing the bubble-induced fluid flow is possible by switching the experimental setup to the tracking of fluorescent nanoparticles seeded into the liquid medium. It is worth noting that no experimental studies of microstreaming induced by a bubble in an infinite liquid exist so far in the literature. Also, even when cavitation microstreaming is investigated for substrate-attached bubble, the analysis is limited to qualitative observations without considering the link to the bubble dynamics[16]. The measurement of particle motion is performed in a thin laser sheet provided by a continuous wave laser. Because it is necessary to perform quasi-simultaneously (i) the laser-nucleation by pulsed laser, (ii) the particle tracking with a laser sheet and (iii) the recording by the high-speed camera, particular attention has to be

paid to the potential obstruction of materials surrounding the water tank. This leads to a compact setup with many restrictions on the devices disposition, as shown in **Figure 5**. When capturing a microstreaming pattern induced by a shape-oscillating bubble, it is necessary to alternatively track the bubble interface dynamics, as mentioned in step 4.2. Indeed, switching between alternative sequences of bubble dynamics and fluid flow visualization allow safely associating the microstreaming pattern to a given shape oscillation. This alternative procedure is mandatory as (i) shape oscillations may turn off, (ii) bubble stability may abruptly increase leading to the positional instability of the bubble, (iii) bubble may fragment when large deformations occur. Even if these events are rare, it is important to verify that the bubble dynamics stays the same by recording it both before and after filming the microstreaming pattern. (In this way it can be assured that the bubble motion and the pattern are really correlated).

Is it evidenced that a bubble oscillating predominantly on a given mode number leads to a particular microstreaming pattern, as shown in **Figure 12**. The pattern is unique and depends on the modal content of the interface motion. As illustrated in **Figure 13**, the same predominant mode number may induce large- or small-distance vortices depending on the number, amplitude, and phase of the secondary modes that are excited.

These observations may have practical use in medical applications such as targeted and localized ultrasound-mediated drug delivery, for instance. Bubbles are known to act as vectors for permeabilizing tight junctions between cells, and even the cell membrane itself, leading to sonoporation[1]. In case of stably oscillating microbubbles, this phenomenon may be induced by the shear stress or shear stress gradients[35] induced by bubble oscillations, through the generation of microstreaming flows. We recall that microstreaming is a nonlinear, second-order phenomenon. At first, scaling the observed streaming patterns to the one obtained for therapeutic, shelled, microbubbles with smaller sizes (~3 µm radius) is not straightforward. We already evidenced in the introduction how nonspherical dynamics of free or coated bubbles of one order of magnitude size difference may be scaled: the eigenfrequency ω_n of a given mode n is related to the bubble size as $\omega_n^2 R_0^2 \sim Constant$[25]. In Dollet et al.[27], shape modes of order 4 have been captured for coated micrometric bubbles excited at 1.7 MHz, similarly to the observed shape mode number in our experiment. Also, the applied pressure strongly differs, as pressure up to 200kPa are required to trigger shape modes on ultrasound contrast agent microbubbles[27]. In the proposed setup, the maximum applied pressure does not exceed 25 kPa. The strong difference in applied pressure results from the triggering of surface instabilities, as shape modes appear above a certain pressure threshold. For the experimental conditions at 1.7 MHz given in Dollet et al. [27], it has been shown that the pressure threshold leading to shape instability is around 150 kPa for a mode 4[36]. For a 30 kHz driving frequency, only a 10 kPa driving field amplitude is required to trigger shape instability on a ~50 µm bubble. Once triggered, the shape instability develops after a few acoustic cycles, and demonstrates a plateau saturation of the mode amplitude. Amplitude saturation was observed for both free bubbles[24,29] and coated bubbles[27]. It indicates the possibility of reaching steady-state shape oscillations for free or coated bubbles, with shape oscillations as large as 25 to 50% of the radial mode amplitude[27,37]. Using our experimental approach, we reach extreme shape deformations in the configuration, $\frac{a_n}{a_0} \sim 3$

(where a_n is the shape mode amplitude), as illustrated in **Figure 13**.

To summarize, the proposed experimental setup allows scaling the main features of nonspherical oscillations of microbubbles, even for sizes varying with almost one order of magnitude. Concerning the microstreaming flow, the scaling of flow velocity may be investigating for bubbles exhibiting both lateral and radial oscillations[38], or a nonspherical mode that is self-interacting[39]. In both cases the streaming velocities scale as $v \sim \omega R_0 a_i a_j$, where i, j denotes the considered mode amplitudes normalized by the bubble radius. For similar values of the nonspherical expansion parameter a_i, identical steaming velocities are obtained when $\omega R_0 \sim Constant$. Comparing our experimental conditions to the one used for therapeutic shelled microbubbles[27], theoretical predictions of streaming velocities differ only from a factor 2.5. Measurements of streaming velocities by particle tracking velocimetry led to estimations of the velocity magnitude of 1mm/s in the here presented setup. This value is similar to the one obtained when investigating microstreaming induced by ultrasound contrast agents[19]. Concerning the spatial organization of the streaming pattern, the angular distribution of the flow vortices around the bubble interface is independent of the bubble radius[31]. Only the radial expansion of the streaming field is impacted by the bubble size modification. This radial expansion scales as $\left(\frac{R_0}{r}\right)^{\alpha}$, where α is a coefficient linked to the investigated mode number. It is clear that the overall shape of the streaming pattern is conserved, as the radial expansion is ruled by the bubble radius R_0. However, as illustrated in **Figure 13**, the streaming pattern can significantly differ even when considering the same shape mode number. **Figure 13** highlights the huge impact of the bubble interface dynamics on the streaming pattern, and particularly on the spatial rate of change in the velocity field. The spatial distribution of shear stress, or shear stress gradient, has been indicated as an appropriate indicator of sonoporation efficiency[35]. In our proposed experimental setup, only the shear stress in the bulk fluid may be assessed at this stage. Further extension to the wall shear stress would require the addition of a nearby surface close to the bubble. It is predictable that a surface in the bubble vicinity will disturb the bubble positional stability by locally modifying the standing wave field. Ensuring bubble stability at a close distance from a wall is still a challenge that may be partly solved by adding a secondary ultrasound field dedicated to bubble trapping with a wavelength identical to the bubble-wall distance. Such a dual-frequency acoustic levitation chamber was already designed for investigating bubble pair dynamics and interaction forces[38]. Unfortunately, the large size difference between the bubbles investigated here and biological cells (typical radius ~10µm) makes the direct use of this experimental setup impossible for biological investigations. However, we expect that our experimental results in combination with the most recent theoretical developments on bubble-induced microstreaming will help improve such modeling, as well as provide confidence in the theoretical prediction of bubble-induced shear stress or shear stress gradients in the vicinity of a cell membrane.

ACKNOWLEDGMENTS:

This work was supported by the LabEx CeLyA of the University of Lyon (ANR-10-LABX-0060 / ANR-11-IDEX-0007).

DISCLOSURES:

The authors have nothing to disclose.

REFERENCES:

1. Roovers, S. et al. The role of ultrasound-driven microbubble dynamics in drug delivery: from microbubble fundamentals to clinical translation. *Langmuir*. **35** (31), 10173-10191 (2019).
2. Liu, H.L., Fan, C.H., Ting, C.Y., Yeh, C.K. Combining microbubbles and ultrasound for drug delivery to brain tumors: current progress and overview. *Theranostics*. **4** (4), 432-444 (2014).
3. Lammertink, B.H.A. et al. Sonochemotherapy: from bench to bedside. *Frontiers in Pharmacology*. **6**, 138 (2015).
4. Lajoinie G. et al. In vitro methods to study bubble-cell interactions: fundamentals and therapeutic applications. *Biomicrofluidics*. **10**, 011501 (2016).
5. Van Amel A., Bouakaz A., Versluis M., de Jong N. Micromanipulation of endothelial cells: ultrasound-microbubble-cell interaction. *Ultrasound in Medicine and Biology*. **30**, 1255-1258 (2004).
6. Tran T.A., Roger S., Le Guennec J.Y., Tranquart F., Bouakaz A. Effect of ultrasound-activated microbubbles on the cell electrophysiological properties. *Ultrasound in Medicine and Biology*. **33**, 158-163 (2007).
7. Marmottant P., Hilgenfeldt, S. Controlled vesicle deformation and lysis by single oscillating bubbles. *Nature*. **423** (6936), 153-156 (2003).
8. Prentice P.A., Cuschieri K., Dholakia K., Prausnitz M., Campbell P. Membrane disruption by optically controlled microbubble cavitation. *Nature Physics*. **1**: 107-110 (2005).
9. Kudo N., Okada K., Yamamoto K. Sonoporation by single-shot pulsed ultrasound with microbubbles adjacent to cells. *Biophysical Journal*. **96**, 4866-4876 (2009).
10. Novell A. et al. A new safety index based on intrapulse monitoring of ultra-harmonic cavitation during ultrasound-induced blood-brain barrier opening procedures. *Scientific Reports*. **10**, 10088 (2020).
11. Cornu C. et al. Ultrafast monitoring and control of subharmonic emissions of an unseeded bubble cloud during pulsed sonication. *Ultrasonics Sonochemistry*. **42**, 697-703 (2018).
12. Reslan L., Mestas J.L., Herveau S., Béra J.C., Dumontet C. Transfection of cells in suspension by ultrasound cavitation. *Journal of Controlled Release*. **142** (2), 251-258 (2010).
13. Reuter F., Gonzalez-Avila S.R., Mettin R., Ohl C.D. Flow fields and vortex dynamics of bubbles collapsing near a solid boundary. *Physical Review Fluids*. **2**, 064202 (2017).
14. Chew L.W., Klaseboer E., Ohl S.W., Khoo B.C. Interaction of two differently sized oscillating bubbles in a free field. *Physical Review E*. **84**, 066307 (2011).
15. Doinikov, A.A., Bouakaz, A. Acoustic microstreaming around a gas bubble. *The Journal of the Acoustical Society of America*. **127** (2), 703-709 (2010).
16. Tho, P., Manasseh, R., Ooi, A. Cavitation microstreaming patterns in single and multiple bubble systems. *Journal of Fluid Mechanics*. **576**, 191-233 (2007).
17. Van Wamel A. et al. Vibrating microbubbles poking individual cells: Drug transfer into cells via sonoporation. *Journal of Controlled Release*. **112**, 149-155 (2006).
18. Helfield B., Chen X., Watkins S.C., Villanueva F.S. Biophysical insight into mechanisms of

sonoporation. *PNAS*. **113** (36), 9983-9988 (2016).
19. Pereno V. et al. Layered acoustofluidic resonators for the simultaneous optical and acoustic characterization of cavitation dynamics, microstreaming, and biological effects. *Biomicrofluidics*. **12**, 034109 (2018).
20. Shklyaev, S., Straube, A.V. Linear oscillations of a compressible hemispherical bubble on a solid substrate. *Physics of Fluids*. **20**, 052102 (2008).
21. Fauconnier, M., Bera, J.C., Inserra C. Nonspherical modes non-degeneracy of a tethered bubble. *Physical Review E*. **102**, 033108 (2020).
22. Xi X., Cegla F., Mettin R., Holsteyns F., Lippert A. Study of non-spherical bubble oscillations near a surface in a weak acoustic standing wave field. *The Journal of the Acoustical Society of America*. **135**, 1731 (2014).
23. Doinikov A.A., Bouakaz A. Effect of a distant rigid wall on microstreaming generated by an acoustically driven gas bubble. *Journal of Fluid Mechanics.* **742**, 425-445 (2014).
24. Cleve, S., Guédra, M., Inserra C., Mauger, C., Blanc-Benon, P. Surface modes with controlled axisymmetry triggered by bubble coalescence in a high-amplitude acoustic field. *Physical Review E*. **98**, 033115 (2018).
25. Lamb H. Hydrodynamics. 6th ed. Cambridge: University Press (1932).
26. Liu Y., Wang Q. Stability and natural frequency of nonspherical mode of an encapsulated microbubble in a viscous liquid. *Physics of Fluids*. **28**, 062102 (2016).
27. Dollet B. et al. Nonspherical oscillations of ultrasound contrast agent microbubbles. *Ultrasound in Medicine and Biology*. **34** (9), 1465-1473 (2008).
28. Versluis M. et al. Microbubble shape oscillations excited through ultrasonic parametric driving. *Physical Review E*. **82**, 026321 (2010).
29. Guédra, M., Cleve, S., Mauger, C., Blanc-Benon, P., Inserra, C. Dynamics of nonspherical microbubble oscillations above instability threshold. *Physical Review E*. **96**, 063104 (2017).
30. Cleve, S., Guédra, M., Mauger, C., Inserra, C., Blanc-Benon, P. Microstreaming induced by acoustically trapped, non-spherically oscillating microbubbles. *Journal of Fluid Mechanics*. **875**, 597-621 (2019).
31. Doinikov, A.A., Cleve, S., Regnault, G., Mauger, C., Inserra, C. Acoustic microstreaming produced by nonspherical oscillations of a gas bubble. I. Case of modes 0 and m. *Physical Review E*. **100**, 033104 (2019).
32. Inserra, C., Regnault, G., Cleve, S., Mauger, C., Doinikov, A.A. Acoustic microstreaming produced by nonspherical oscillations of a gas bubble. III. Case of self-interacting modes n-n. *Physical Review E*. **101**, 013111 (2020).
33. Prabowo, F., Ohl, C.D. Surface oscillations and jetting from surface attached acoustic driven bubbles. *Ultrasonics Sonochemistry*. **18** (1), 431-435 (2011).
34. Garbin, V. et al. Changes in microbubble dynamics near a boundary revealed by combined; optical micromanipulation and high-speed imaging. *Applied Physics Letters*. **90**, 114103 (2007).
35. Collis J. et al. Cavitation microstreaming and stress fields created by microbubbles. *Ultrasonics*. **50**, 273-279 (2010).
36. Loughran J., Eckersley R.J., Tang M.X. Modeling non-spherical oscillations and stability of acoustically driven shelled microbubbles. *The Journal of the Acoustical Society of America*.

131 (6), 4349-4357 (2012).
37. Vos H.J., Dollet B., Bosch J.G., Versluis M., de Jong N. Nonspherical vibrations of microbubbles in contact with a wall – a pilot study at low mechanical index. *Ultrasound in Medicine and Biology*. **34** (4), 685-688 (2008).
38. Regnault G., Mauger C., Blanc-Benon P., Inserra C. Secondary radiation force between two closely spaced acoustic bubbles. *Physical Review E*. **102**, 031101 (2020).

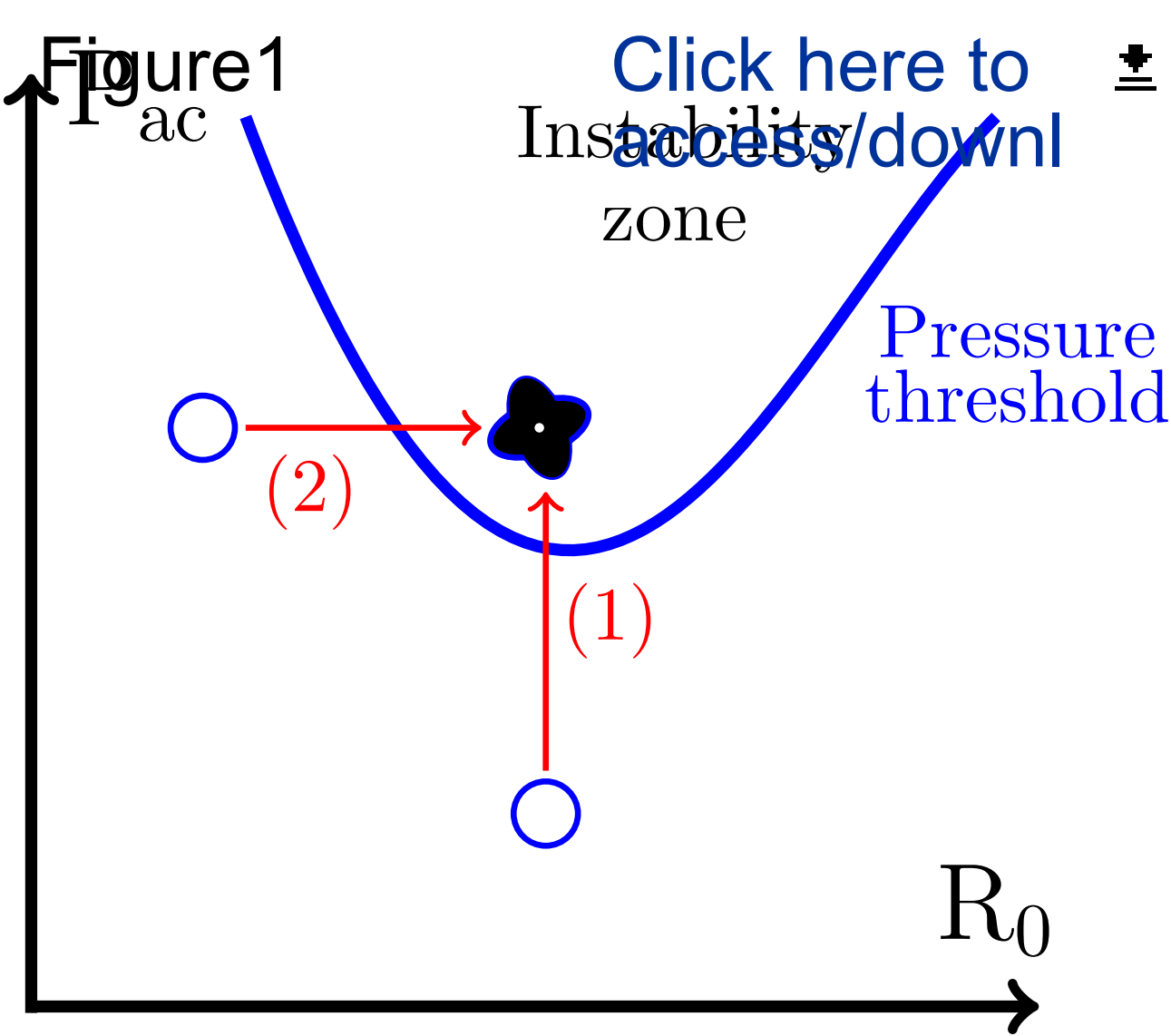

Figure2

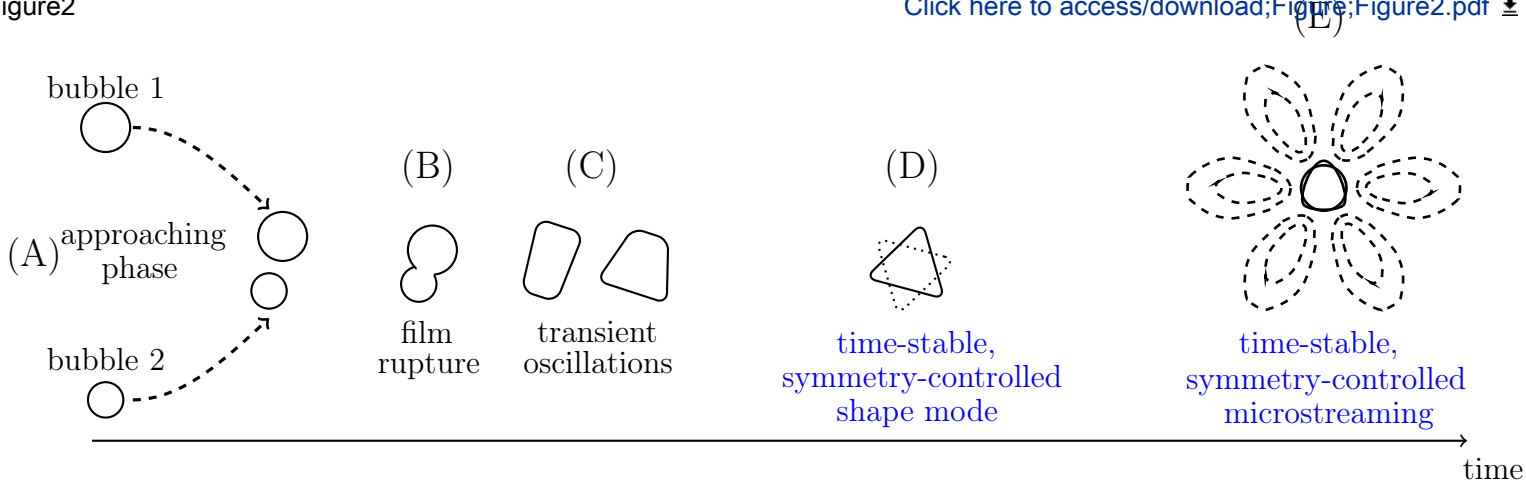

Figure3

Click here to access/download;Figure;Figure3.pdf

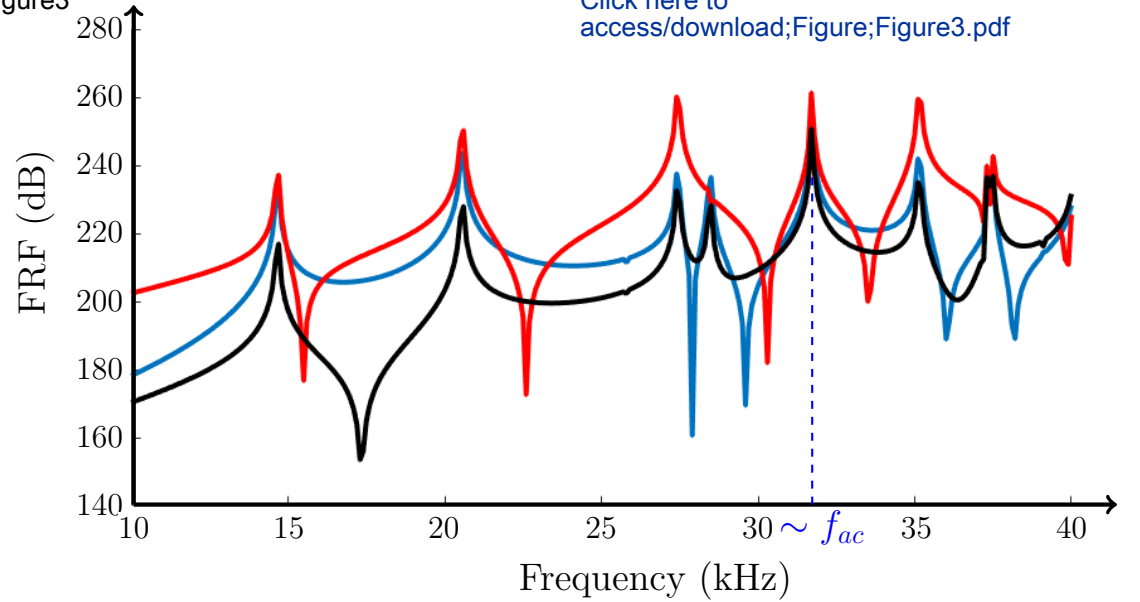

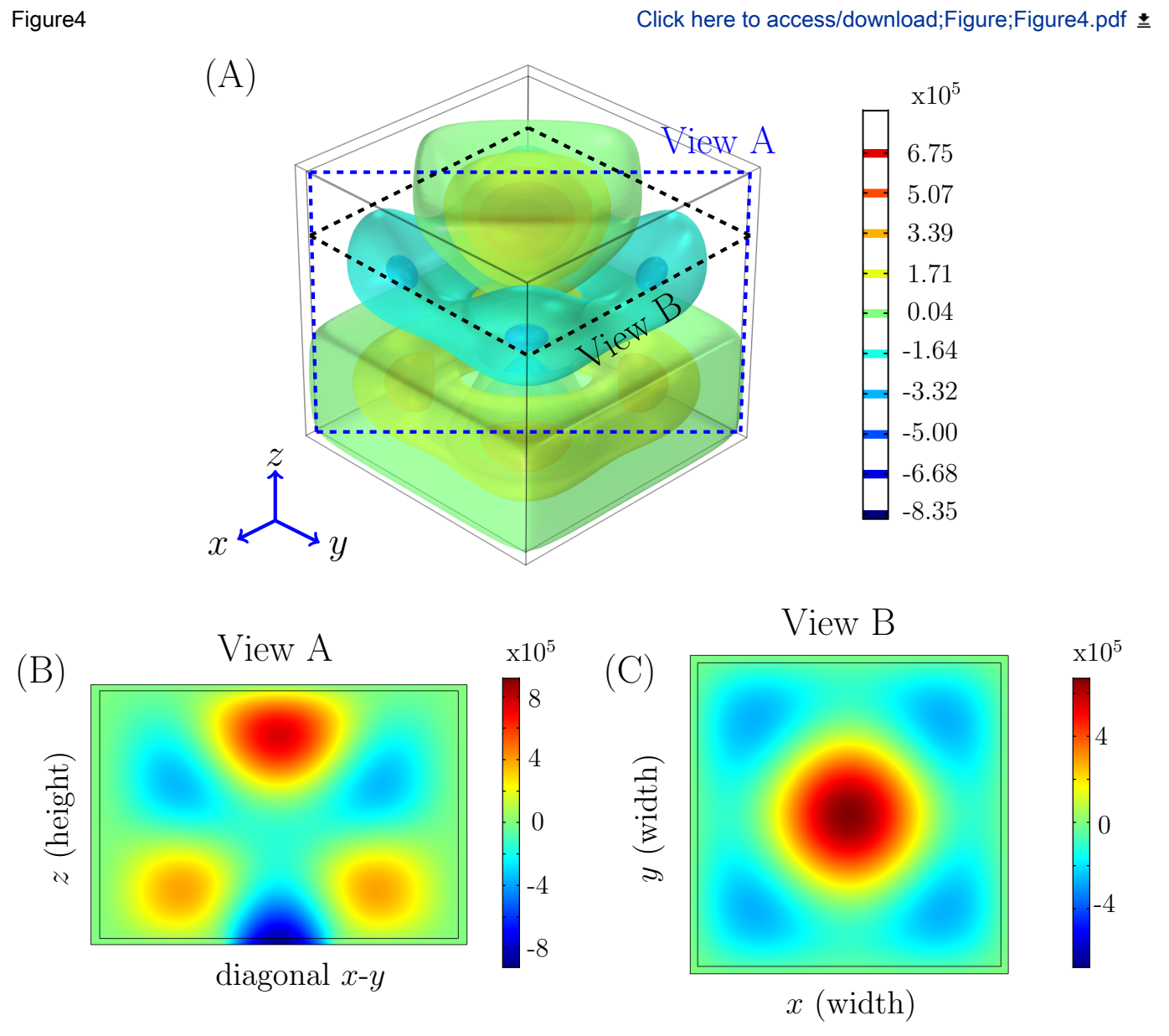

Figure5

Click here to access/download;Figure;Figure5.pdf

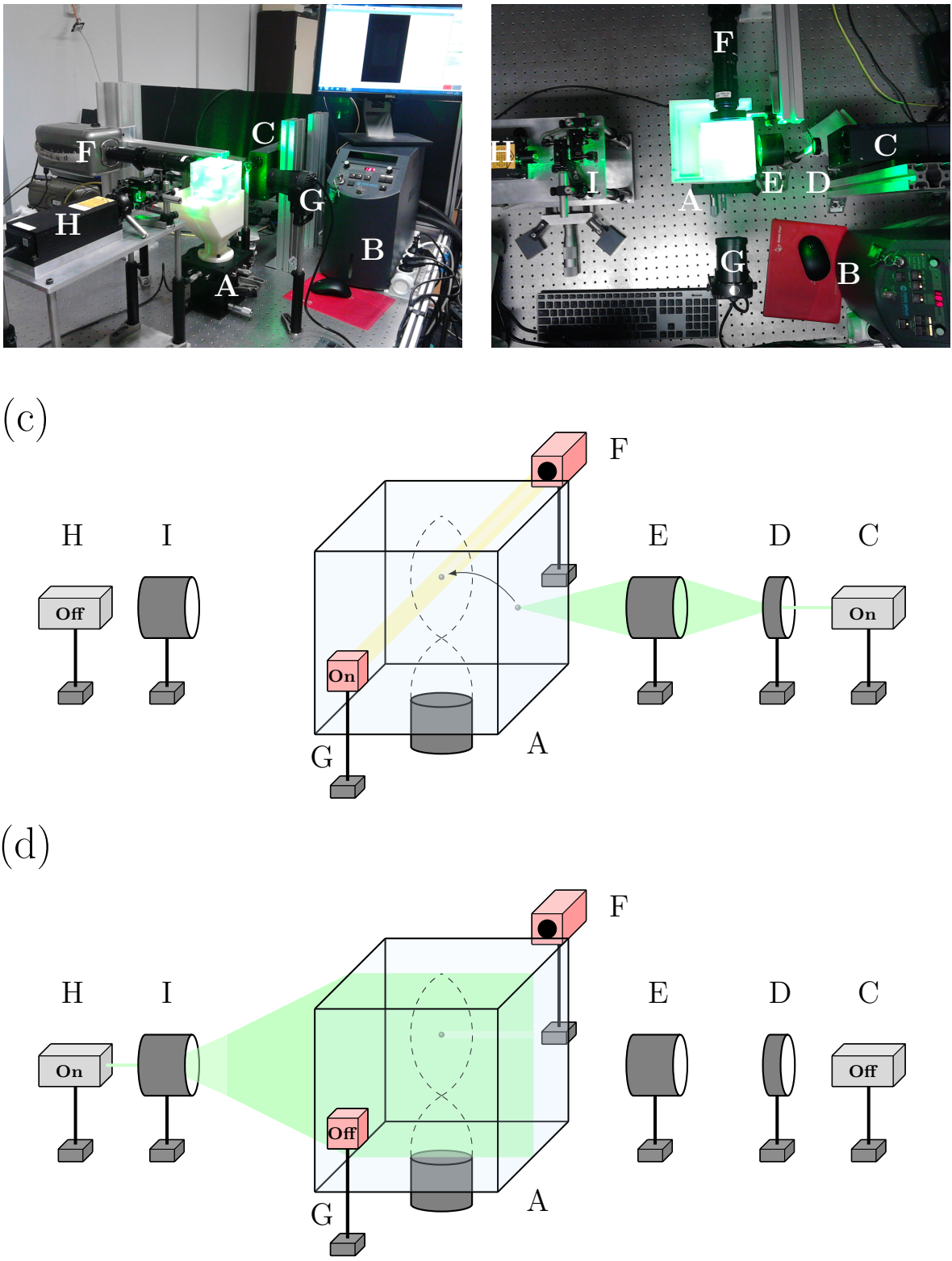

Figure6

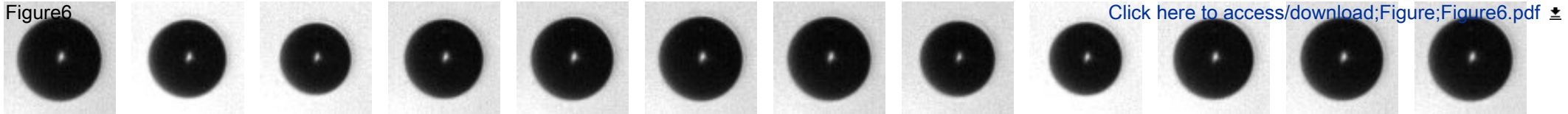

Figure7

Interface_tension_pression

(A)

Physical parameters

frame rate
180064

Vaporized pressure
2330

Excitation frequency
31250

Bulk density
998

Kapa
1.4

Pixel size
2.95

Sound speed
1480

Static pressure
100000

Surface tension
0.0728

Viscosity
0.001

Voltage/Pressure relationship

Bubble radius analysis

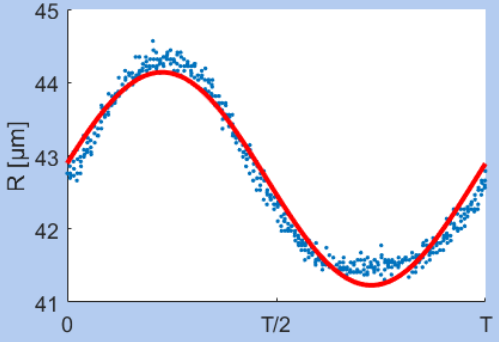

Load parameters

(C)

Auto

Next

R0 [μm]

42.68

(D)

Pressure(Voltage) graph

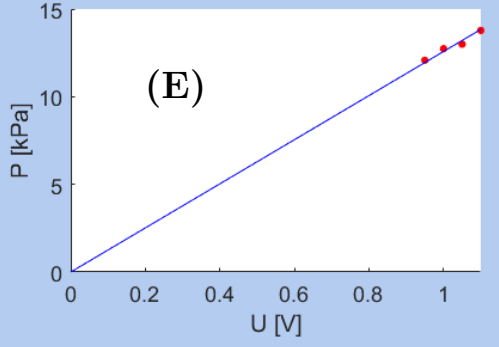

Linear regression

slope

12578

	Voltage	Pressure
1	1.1000	13778
2	1.0500	12997
3	1	12738
4	0.9500	12079
5	0.9000	0
6	0.8500	0
7	0.8000	0
8	0.7500	0
9	0	0
10	0	0

(B)

Figure8

Click here to access/download;Figure;Figure8.pdf

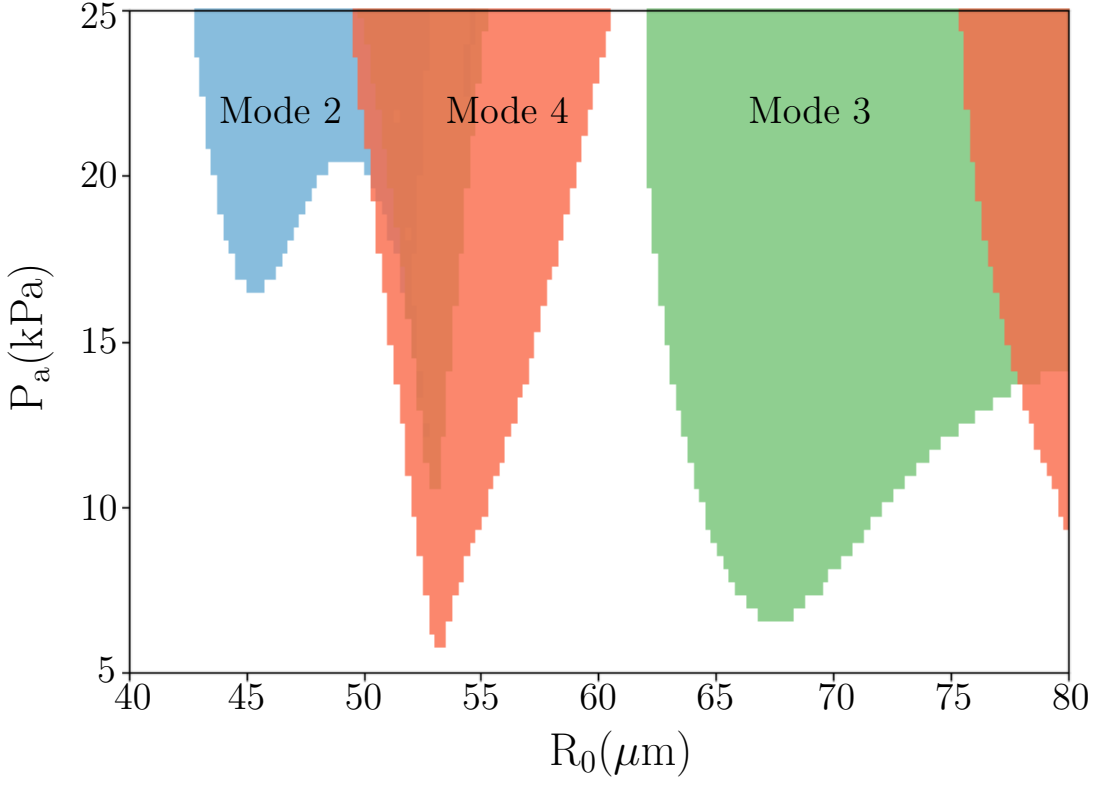

Figure9

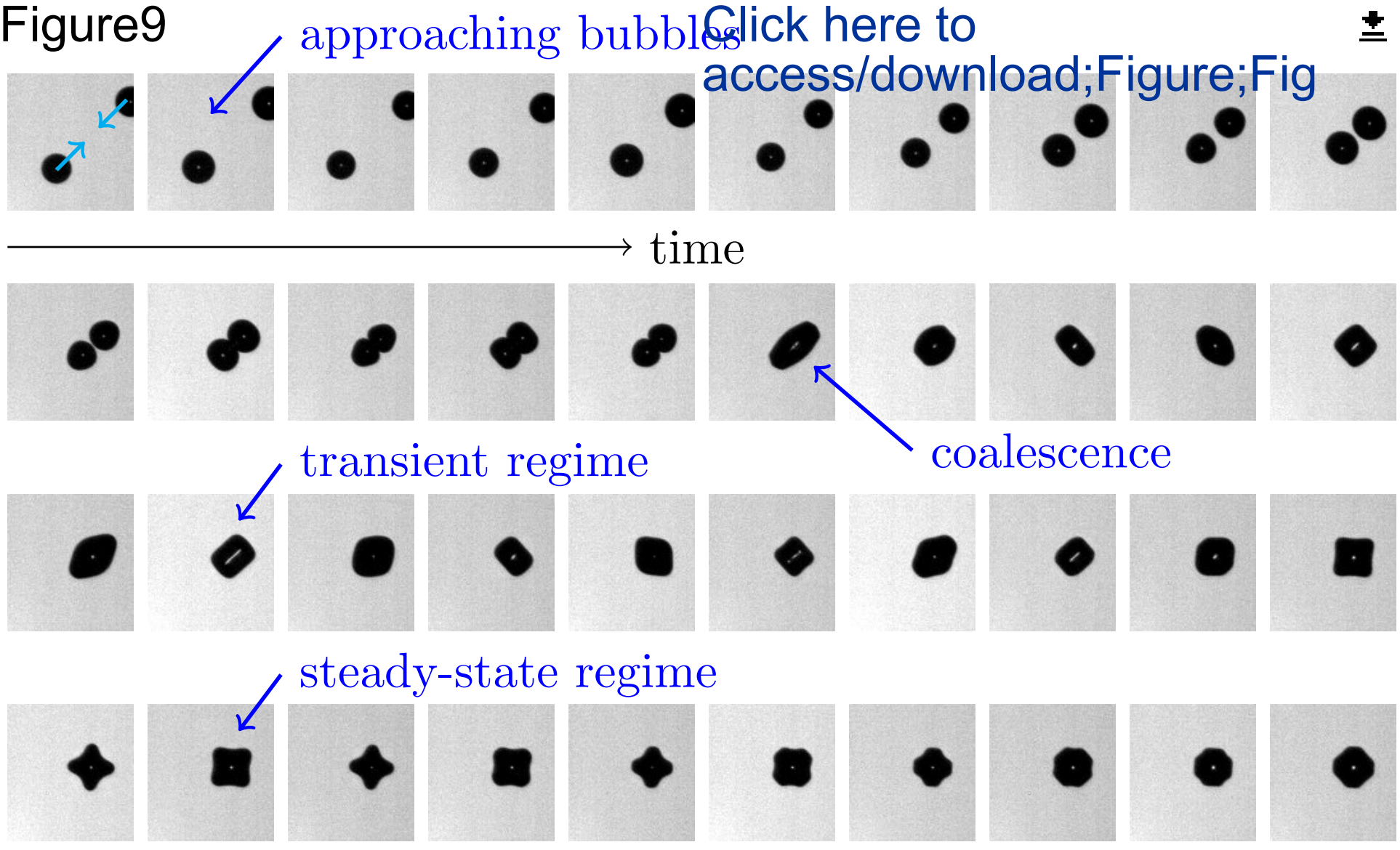
approaching bubbles
Click here to access/download;Figure;Fig
time
coalescence
transient regime
steady-state regime

Figure10

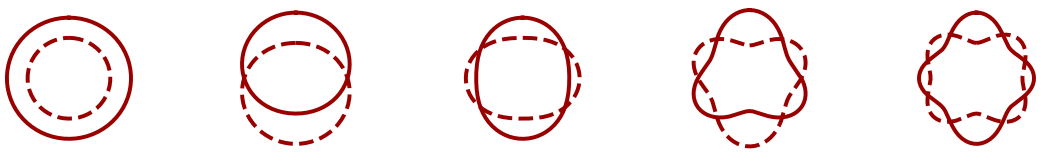

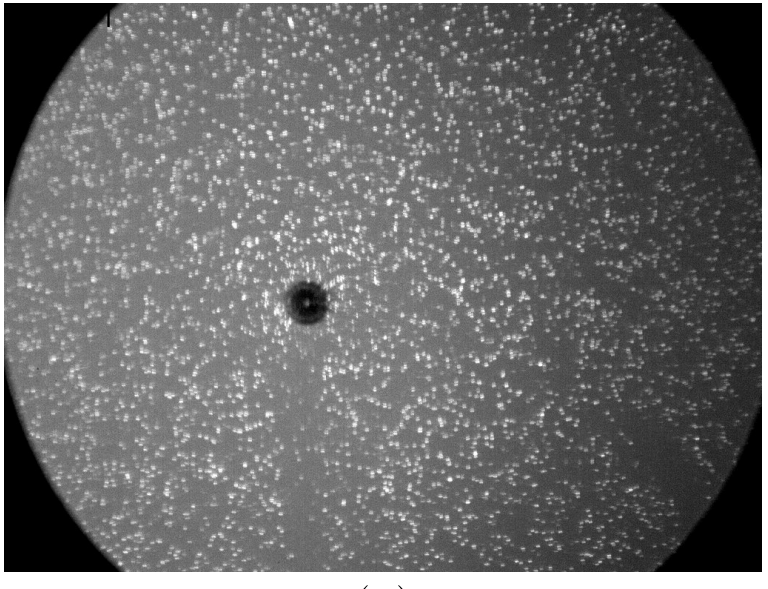

(a)

(b)

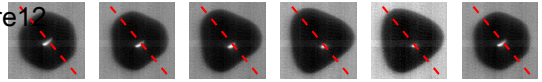

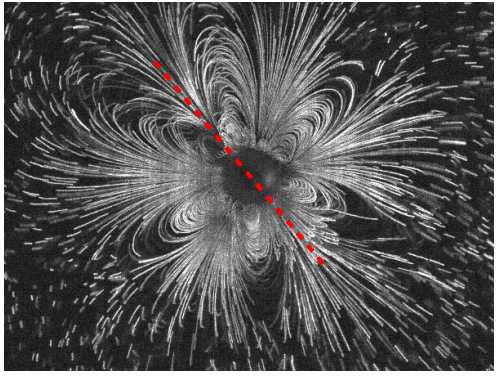

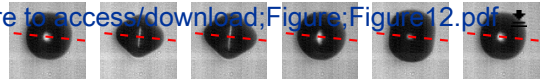

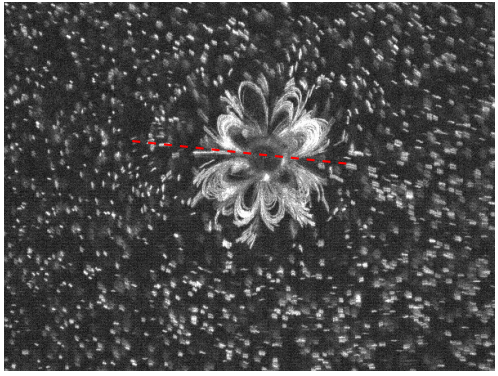

Figure13

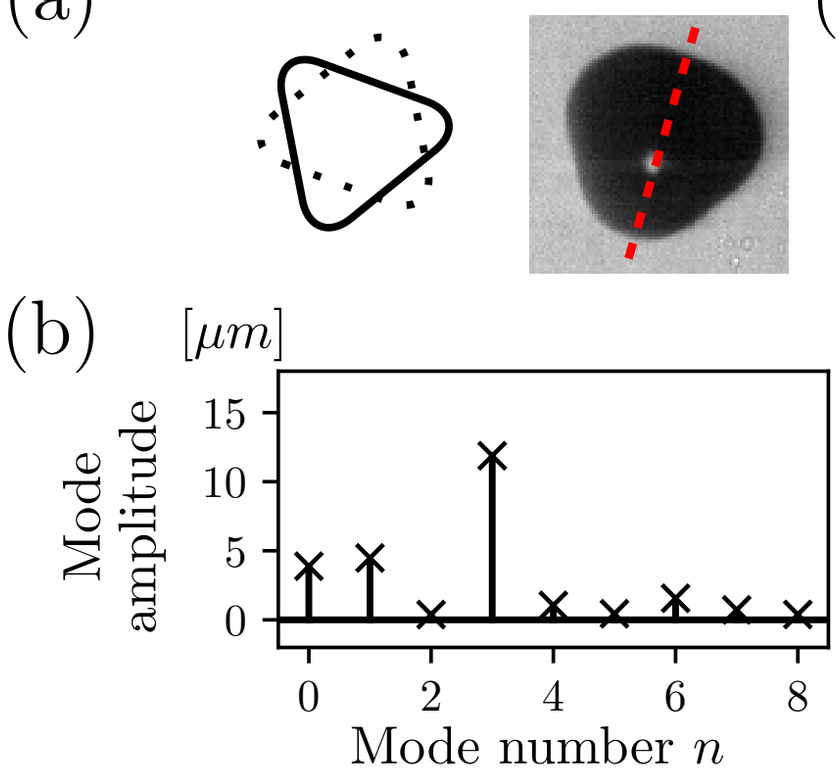

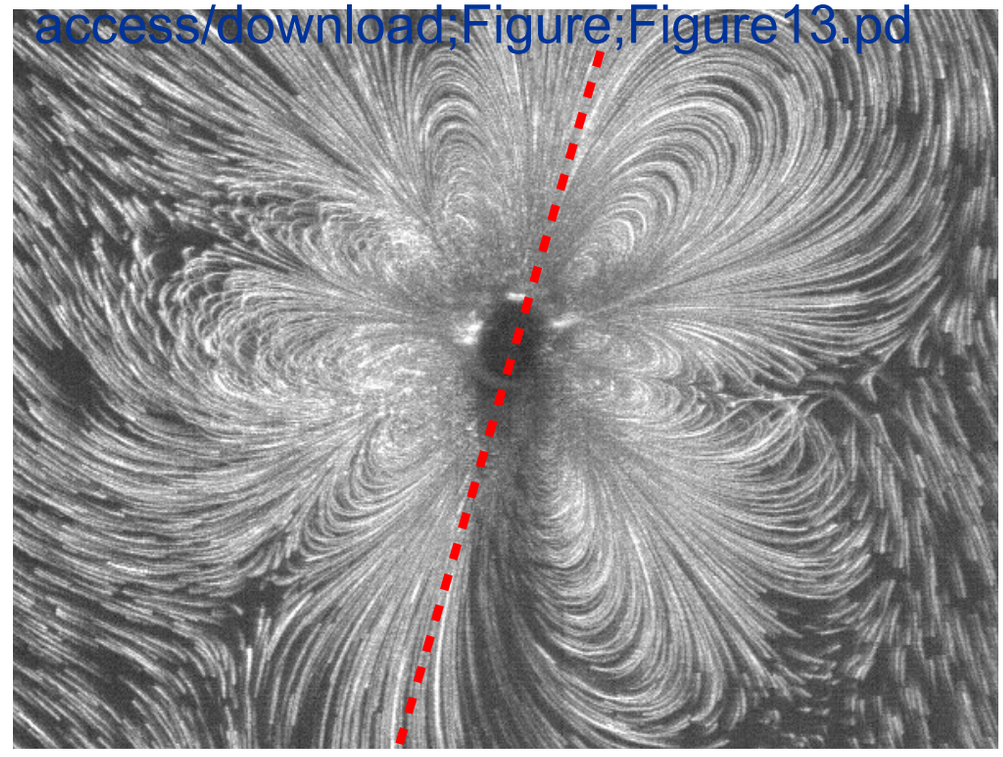

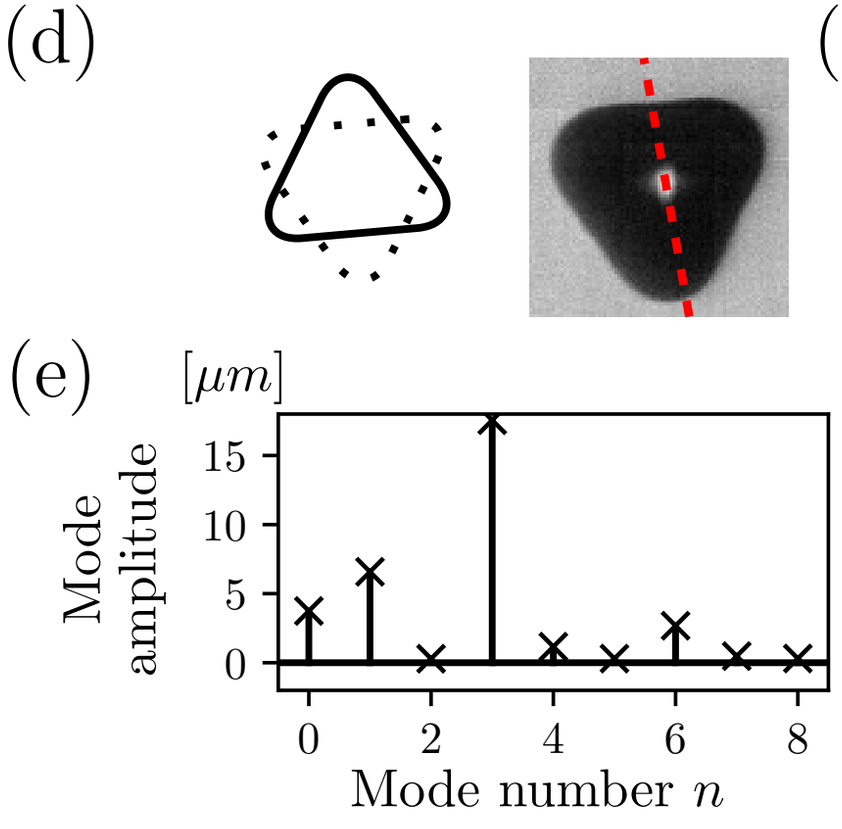

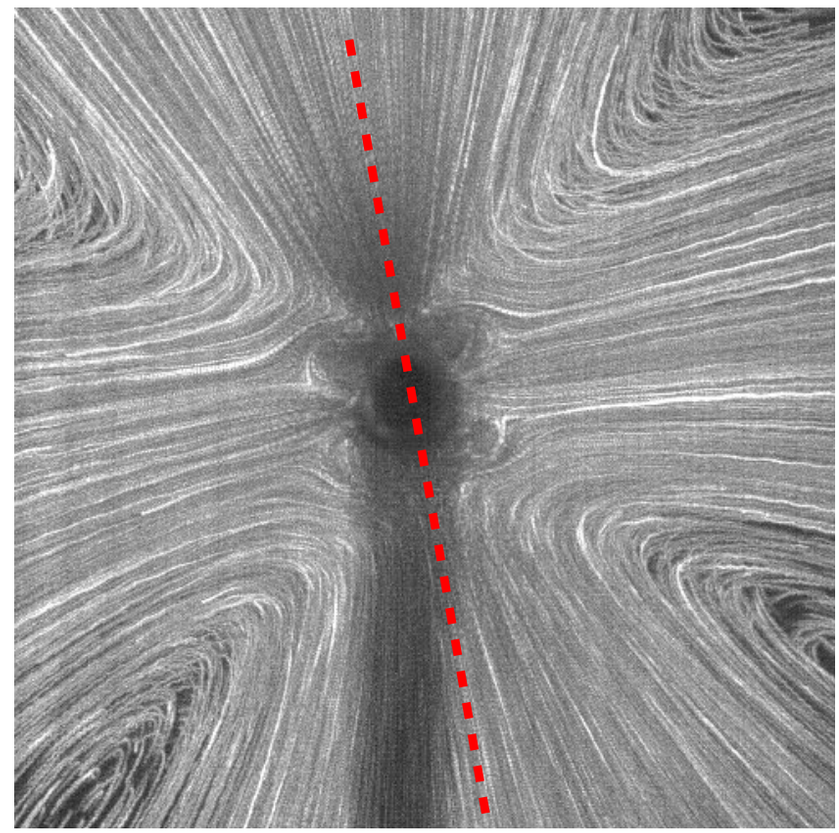

Name of Material/Equipment	Company	Catalog Number	Comments/Description
Aspherical lens	Thorlabs	AL4050	Lens of focus 40 mm
Continuous wave laser source	CNI	MLL6FN	DPSS laser of wavelength 532nm, energy 400 m\
Cylindrical plano-concave lens	Thorlabs	LJ1277L1-A	lens of focus -25?4mm
Cylindrical plano-concave lens	Thorlabs	LK1900L1	lens of focus 250 mm
Fluorescent particles	Duke Scientific	R700	Red polymer fluorescent microspheres
Function generator	Agilent	HP33120	Generator of function feeding the ultrasound tra
High-speed camera	Vision Research	Phantom v12.0	High-speed recording up to 1 Mfps
Liquid medium	Carlo Erba	Water for analysis	Demineralized, undegassed water
Multiphysics software	Comsol	None	Softwate for simulating the acoustic field of the
Nd:Yag pulsed laser	New Wave Research	Solo III-15	5 ns pulse duration, λ=532 nm, 3.5 mm beam dia
Plano-concave lens	Thorlabs	N-BK7	lens of focus 125 mm
Spherical concave lens	Thorlabs	N-SF11	Bi-concave lens of focus -25mm
Ultrasound transducer	SinapTec	Custom-made	Nominal frequency 31kHz, active area 35mm dia
Visualization software	NIH	ImageJ	Software for image processing and analysis in Ja\
XY Linear stage	Newport	M-406	Displacement stage with micrometric screw
Z-axis linear stage	Edmund Optics	62-299	Vertical displacement stage with micrometric scı

N

ansducer

levitation chamber

ameter, up to 50 mJ

meter
va

rew

Manuscript ID: JoVE62044
Title: Investigating nonspherical bubble oscillations and its induced microstreaming in an acoustic levitation system
Authors: Claude Inserra, Gabriel Regnault, Sarah Cleve, Cyril Mauger, Philippe Blanc-Benon

We thank the Referees for their constructive criticism. The manuscript has been revised to address all the comments of the Referees.
Below we reproduce the Referees' comments and describe our response to them.

Editorial Comments

Changes to be made by the Author(s):

1. Please take this opportunity to thoroughly proofread the manuscript to ensure that there are no spelling or grammar issues. Please define all abbreviations at first use.

Done

2. Please shorten your title to "Induction of Microstreaming by Nonspherical Bubble Oscillations in an Acoustic Levitation System".

Done

3. JoVE cannot publish manuscripts containing commercial language. This includes trademark symbols (™), registered symbols (®), and company names before an instrument or reagent. Please remove all commercial language from your manuscript and use generic terms instead. All commercial products should be sufficiently referenced in the Table of Materials and Reagents.
For example: COMSOL Multiphysics®; Carlo Erba®; Langevin-type Reson®; etc

Done. We have modified the Table of Materials in consequence.

4. The Protocol should be made up almost entirely of discrete steps without large paragraphs of text between sections. Please simplify the Protocol so that individual steps contain only 2-3 actions per step and a maximum of 4 sentences per step.

Done. We have simplified the steps in Protocol-Part I. Deleting commercial language considerably simplified Protocol 2.1. We have deleted the long notes in Protocol-Part II and III.

5. Please note that your protocol will be used to generate the script for the video and must contain everything that you would like shown in the video. Please add more details to your protocol steps. Please ensure you answer the "how" question, i.e., how is the step performed? Alternatively, add references to published material specifying how to perform the protocol action. Please add more specific details (e.g. button clicks for software actions, numerical values for settings, etc) to your protocol steps. There should be enough detail in each step to supplement the actions seen in the video so that viewers can easily replicate the protocol.

Done. We have particularly modified Protocol-Part I about the simulation of the acoustic field, in order to clarify the required steps to obtain numerical data;

6. Section 1: What are the dimensions of this tank? How do you design it? If this is not part of the video, please cite a reference. How do you simulate the FRF? How do you plot the pressure field inside the tank?

Done. We have modified Protocol-Part I in order to clarify how to obtain numerical data.

7. After including a one-line space between each protocol step, make sure that up to 3 pages of protocol text are highlighted for inclusion in the protocol section of the video. This will clarify what needs to be filmed.
Done. Highlighted protocol text reaches 2.5 pages with one-line spacing between steps.

As we are a methods journal, please add to the Discussion with citations:

a) Any limitations of the technique

We have added a paragraph in the Discussion part in order to address this point.

b) Any future applications of the technique

We have added a paragraph in the Discussion part in order to address this point.

8. Please sort the Materials Table alphabetically by the name of the material.

Done.

Referee 1

Manuscript Summary:

In thıs work, a new method is proposed to control the oscillation modes of a single, trapped acoustic bubble and is based on coalescence technique between two bubbles. The steady-state, symmetry-controlled bubble shape oscillations allow analyzing the fluid flow generated in the vicinity of the bubble interface. They show that even the high-order oscillation modes can induce long-range fluid circulation if the interface dynamics contains several modes, highlighting the applications of nonspherical oscillations potentially for site specific drug delivery.

Minor Concerns:

I have no concerns. Overall, the manuscript is well-written and easy to follow. The manuscript concisely and clearly describes an acoustofluidic method for utilizing higher oscillation modes of microbubbles.

Thank you for your positive comments.

Referee 2

Manuscript Summary:

In this manuscript the authors present an experimental protocol for the controlled seeding of non-spherical (high mode content) oscillations of laser-nucleated bubbles in water. The study is well-motivated since it has been suggested that the resulting oscillation-induced streaming may be responsible for increased permeability of the cell membrane, leading to enhanced absorption of drugs. To date, a method for stimulating non-spherical oscillations in isolated bubbles away from surfaces that affect the resulting flow pattern has been missing, and therefore this manuscript is a useful addition to the field. It should be noted that the manuscript describes the protocols for stimulating non-spherical oscillations and observing the resulting microstreaming patterns, not measuring increases in drug absorption, but this in no way lessens the significance of the manuscript since, as described, controlling and imaging the bubble oscillations is in itself highly challenging.

Major Concerns:
None

Minor Concerns:
The protocol as written gives a clear description of the steps required for successfully reproducing the results shown here, and is well-suited for publication in JoVE. There are some relatively minor points the authors may address:

1. Protocol step 1.1. At the very first step it would be useful to give more information about constraints and considerations for the tank design, even, e.g. the volume of water contained

We have added more information in the manuscript about tank design. Instead of only furnishing the details for our homemade designed water tank, Protocol-Part I is dedicated to the design of a water tank for any choice of the driving frequency. Because the ultrasound transducer is located at a tank wall through echograhic gel, there is no particular constraint on the tank design, except a movable top face in order to fill the tank in an easy way.

2. Protocol step 3. Are any parts of this step automated, or do they require the intervention of the user in identifying bubbles and adjusting experimental parameters?

This part is not automated, as the multiple coalescence technique requires an initially-undefined number of multiple laser sparks. After some experiments, the user knows well which parameters should be modified in order to obtain the desired results. The only three parameters to adjust are: the amplitude of the driving ultrasound wave, the number and amplitude of sparks. Using real-time bubble analysis, automation is indeed possible. However, we do not believe in a significant time gain by doing so.

3. Protocol step 4.1. It would be more useful to give an (approximate) number density of fluorescent microparticles to use

We have indicated the approximated number density of particles, set to ~4.10^4 particles/mm^3 in our configuration.

4. Protocol step 4.5. What sort of "movable" device is the laser mounted on (e..g in step 2.1 manufacturer and part codes of apparatus are given). Does the whole laser need to move, or can the beam be steered with mirrors?

The laser is not movable. The laser head, as well as the lenses are fixed. In this way, the location of the laser spark is well defined in space. Thus, we locate the acoustic levitation chamber, that includes the {water tank + ultrasound transducer} put atop a three-displacement table (the movable device). Thus, only the relative location of the laser spark within the water tank, meaning within the spatial acoustic field, is adjustable with the displacement table. To clarify this point, we moved the whole description of the acoustic levitation chamber within Protocol-Part I, including the movable displacement table. In Protocol-Part II, only remains the setting of the laser path with lenses for bubble nucleation.

Referee 3

Manuscript Summary:

The authors reported their studies on acoustically oscillating bubbles. I think this work is innovative. First of all, to detect the oscillating nonspherical bubbles, the authors developed the levitation and coalescence techniques. Second, the authors systematically studied the fluid patterns and shear stresses induced by the modal content of the bubble interface. Thirdly, the authors may provide some unique insights for the ultrasound-based drug delivery. The results make scenes, and the manuscript is well written. I think this is very high-quality work. Thus, I recommend accepting this work as it is.

Thank you for your positive comments.

Referee 4

The paper by Inserra and co-authors describes an experimental method based on acoustic levitation, to investigate nonspherical bubble oscillations and induced microstreaming. The method provides an interesting contribution to the study of cavitation microstreaming, which is a process implicated in ultrasound-mediated drug delivery. It is recommended that the following comments are addressed prior to consideration for publication.

ABSTRACT
- Authors may consider using the term "cavitation microstreaming" to qualify microstreaming induced by a cavitating microbubbles. The term "acoustic microstreaming" is often employed in the literature to describe streaming induced by ultrasound alone within a microfluidic cavity. Otherwise, they could also clarify their terminological choices at the beginning of the manuscript.

It is true that terminology matters, and we usually refer to “acoustic streaming” for the flow induced by the ultrasound alone, whatever the environment (microfluidics or not). In order to alleviate any misunderstandings, I modified the mention to the flow induced by the bubbles to “cavitation microstreaming”, as proposed.

- It is recommended that authors include some key quantitative values for relevant parameters used in the study (i.e., US pressure and frequency, microbubble size, etc.).

We have added supplementary quantitative information (bubble size from 30 to 80 µm, typical applied pressure from 0 to 25 kPa, ultrasound frequency set to 31.2 kHz).

INTRODUCTION

- It is recommended that authors elaborate more in detail on the reasons limiting drug penetration within a target tissue, and the ways in which cavitation microstreaming may overcome these.

We have modified the Introduction in order to highlight how cavitation microstreaming may appear as the best candidate for an optimal efficiency for cell membrane permeabilization, as a function of the targeted therapeutic application.

- Authors state that "drugs are either co-injected into a gas bubble". Do they mean "that free drugs can be co-injected with a gas bubble suspension"?

Indeed. We have modified this sentence.

- Authors mention that "capturing the dynamics of cells in response to bubble-induced mechanical stimuli is very difficult." It is recommended that they elaborate more on the key technological challenges associated with it. Is their proposed system suitable to address all (or some) of these challenges? These aspects could be address in the Discussion section too. The manuscript would benefit from a more critical assessment of the benefits and limitations of the proposed method, with more explicit reference to others proposed in the literature.

We have modified the Introduction and Discussion in order to address these points.

- Authors state that "the second barrier is how to control the collapsing bubble regime to avoid microbubble-induced cell lysis." I would suggest to first describe the ideal properties of an ultrasound-mediated treatment method, to clarify why a collapsing regime may not be indicated in some cases (or in which applications it could instead be exploited).

We have modified the Introduction in order to address these points, focusing on the sensitive therapeutic application in which side effects of collapsing bubbles should be avoided.

- In addition to the shear stress magnitude, authors should also refer to the spatial gradients of shear stress as a determinant of cell membrane permeabilization. It should also be clarified whether they are referring to wall shear stress (WSS) in some instances.

We have added mention to shear stress gradients, and took care of the use if shear stress versus WSS.

- Authors seem to suggest that prior studies are limited to the condition of microbubbles attached to a surface. Prior to these considerations, they should provide a clearer description of a therapeutically relevant model or scenario. For instance, there may be conditions whereby bubbles are actively targeted to a specific tissue. They should also explain more clearly why

they consider a bubble in suspension to be more reflective of a therapeutic scenario than a bubble located in proximity to a substrate?

We do not claim that the free (far from boundary) bubble scenario is the most suitable for in-vivo applications. Indeed, depending on the targeted application, either bubbles free to move in large vessels or bubbles attached to cells might be favored. When considering therapeutic applications such as in-vitro cell transfection, a collection of cells and bubbles are suspended in a sonicated medium. In this case, the condition of bubbles that are far from boundaries, in almost isotropic conditions, well reflects what is happening in the transfection chamber. Here, we choose to study the bubble shape instabilities and induced microstreaming because of the existence of theoretical models that would allow to confront our experimental data. For substrate-attached bubbles, even the bubble shape dynamics is a complicated matter, and greater are the problems linked to a proper understanding of the liquid flows. This is due to the 3D, non-axisymmetric nature of the shape oscillations in this case. To the best of our knowledge, this is an unsolved problem in the literature.
We modified the introduction in order to better describe the choice of the current configuration.

- It is recommended that authors cite and discuss other recent studies in this area, which didn't employ targeted microbubbles (for example: Pereno et al., Biomicrofluidics, 12, 034109 (2018)).

Done.

- Authors state that "In particular, shape oscillations of microbubbles have to be triggered and kept stable. Furthermore, the orientation of the bubble shape oscillations has to be controlled…". It would be recommended to discuss how these oscillation modes could be induced and controlled in vivo.

For in-vivo applications and when using ultrasound contrast agents, these oscillations modes would naturally be excited once the pressure threshold is exceeded. We modified the Discussion to address this point. We have provided orders of magnitude for triggering such shape instabilities on coated microbubbles. The control of the shape oscillations is an important matter when investigating the bubble contour and the induced liquid flow. So, it matters when performing fundamental studies. For applications, such control is not mandatory: once the shape instability is triggered, cavitation microstreaming would occur with a particular pattern which will impact the surrounding medium around the bubble.

- Authors should also discuss the typical ranges of acoustic pressures, US frequencies, and microbubble dimensions that are employed in ultrasound-mediated drug delivery. How do their experimental conditions compare with these parameter values?

We have modified the Introduction, in order to highlight how a scale analysis can be performed on the investigation of nonspherical oscillations for uncoated/large and coated/small bubbles.

PROTOCOL and DISCUSSION:

We have added a paragraph in the Discussion part in order to discuss the following points 1, 2 and 4 (effect of bubble size, coating, frequency/pressure).

- The bubble dimensions used in this study appear to differ from the ones of shelled microbubbles used in drug delivery applications. Authors should provide a justification for their choice. Moreover, are the findings reported in this study generalizable to clinically relevant microbubble sizes? Could their system be used to evaluate these conditions too?

We have added a paragraph in the Discussion part in order to address this point.

- Microbubbles employed in drug delivery applications are typically coated with a surfactant layer. It would be recommended to discuss about the lack of coating in this study, and potential implications.

We have added a paragraph in the Discussion part in order to address this point.

- Authors mention that 0.71 μm particles are acoustically transparent. Do they mean that the acoustic radiation forces on these particles would be significantly smaller than liquid drag forces?

By acoustically transparent, we mean that particles are small enough not to be influenced by the acoustic radiation force (our particles are ten time smaller than the critical size for their motion being impacted by this force). They also have an inertial behavior, a condition that is fulfilled if the Stokes number of the particle is much smaller than 1. We modified the manuscript in order to clarify the meaning of acoustically-transparent.

- Authors should comment on the US frequency and pressures used. How do they compare to the ones more commonly used in drug delivery applications of US and microbubbles?

We have added a paragraph in the Discussion part in order to address this point.

- Could the proposed system be used to perform a quantification of streaming velocity and induced shear stress? I would suggest commenting on this potential aspect.

We have added a paragraph in the Discussion part in order to address this point.

Click here to access/download

Supplemental Coding Files

VoltagePressure.exe